

The Effect of Uncouplers of Oxidative Phosphorylation on Lipid Bilayer Membranes: Carbonylcyanide *m*-Chlorophenylhydrazone

OLIVER H. LEBLANC, JR.

General Electric Research and Development Center,
Schenectady, New York 12301

Received 14 October 1970

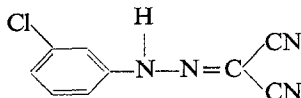
Summary. Detailed experimental data for conductivity and membrane potentials are presented for lecithin/cholesterol/decane bilayers in the presence of the uncoupler carbonylcyanide *m*-chlorophenylhydrazone (CCCP). These compare favorably with a theoretical model derived to explain the mechanism of action of uncouplers on bilayers. The model assumes that the weak acid uncoupler HA and its anion A^- are the sole species which permeate the membrane. Its key feature is the recognition of the existence of unstirred aqueous layers on either side of the membrane. The model accounts for, among other things, a maximum in the transmembrane conductivity at a pH to the alkaline side of the uncoupler pK_a and saturating current-voltage characteristics at high pH, both phenomena being found for CCCP. From a quantitative fit of model to data, values of 2.0×10^{-3} and 11 cm/sec are deduced for the permeability coefficients of the CCCP anion and the undissociated CCCP molecule, respectively.

Certain weak acids, also known to be uncouplers of oxidative phosphorylation in mitochondria and chloroplasts, induce pH-dependent conductances and membrane potentials in lipid bilayer membranes (Bielawski, Thompson & Lehninger, 1966; Skulachev, Sharaf & Liberman, 1967; Hopfer, Lehninger & Thompson, 1968; Liberman, Mochova, Skulachev & Topaly, 1968; Liberman & Topaly, 1968*a, b*; Liberman & Babakov, 1968; Babakov, Demin, Sokolov & Sotnikov, 1968). The mechanism of action of uncouplers on lipid membranes is of some interest, particularly since their behavior in bilayers was in a sense predicted by the mode of action suggested for them in mitochondrial and chloroplast membranes by the chemiosmotic theory of oxidative phosphorylation (Mitchell, 1966).

This paper represents an experimental and theoretical attempt to explore the mechanism of uncoupler action on bilayers. On the experimental side, rather than making a few measurements for a number of different uncouplers, we have chosen to concentrate on a single uncoupling agent,

trying to obtain for it a set of data as complete as possible to compare with theory.

We chose the particular agent carbonylcyanide *m*-chlorophenylhydrazon (CCCP),



first described by Heytler and Pritchard (1962), because we had a good sample available, but primarily because its acid dissociation constant is such that with this compound the full pH range of interest is experimentally convenient.

It remains for further work to prove or disprove if CCCP is indeed a good model compound for the whole class of uncoupling agents, but we propose that the mechanism described in this paper is applicable to all uncoupling agents so far examined in bilayer experiments (with probably one notable exception). More generally, we propose that this mechanism is applicable to a larger class of ion-carrier membrane systems, i.e., where there is a simple one-to-one stoichiometry between ion and carrier, and where either the carrier or the ion-carrier complex is uncharged.

The exceptional case for the uncouplers is that of the substituted benzimidazoles (Lieberman *et al.*, 1968; Lieberman & Topaly, 1968*b*). For these compounds, the stoichiometry is different. The mechanism is probably that arrived at independently by Lea and Croghan (1969) and by Finkelstein (1970), in which the principal ionic species transported through the membrane is a complex, AHA^- , of the weak acid uncoupler HA and its anion A^- . According to this scheme, the observed transmembrane conductivity varies as the square of the total uncoupler concentration, and the conductivity has a maximum at an aqueous pH equal to the pK_a of the uncoupler. The benzimidazoles exhibit these phenomena.

In contrast, we find for CCCP a conductivity which varies directly with uncoupler concentration and which exhibits a maximum at a pH to the alkaline side of the uncoupler pK_a . A linear dependence on uncoupler concentration is also displayed by the data of Lieberman and Topaly (1968*b*) for a great variety of uncouplers other than benzimidazoles. And although they found the conductivity maximal at pH's very near the uncoupler pK_a 's, Hopfer *et al.* (1968) also reported a maximum well to the alkaline side of pK_a for the uncoupler carbonylcyanide *p*-trifluoromethoxyphenylhydrazone.

As we demonstrate here, these electrical phenomena, and others, are consistent with a mechanism in which the principal species transported

through the membrane are the uncoupler itself, HA, and its anion, A^- . This model was previously considered by Markin, Krishtalik, Liberman and Topaly (1969) and by Markin, Pastushenko, Krishtalik, Liberman and Topaly (1969).

The principal difference between our work and theirs is the explicit consideration of two additional features which are essential to dispose of the phenomena. First, the presence of unstirred aqueous layers on either side of the membrane is taken into account. Second, it is recognized that the permeability of the uncharged species HA through the lipid membrane must be orders of magnitude greater than that of the charged species A^- .

Materials and Methods

The sample of carbonylcyanide *m*-chlorophenylhydrazone (CCCP) was a gift from Dr. George M.J. Slusarczuk, who prepared it by the method of Heytler and Pritchard (1962). Metachloroaniline was diazotized with NaNO_2 in aqueous HCl, neutralized with NaHCO_3 , and coupled with malonitrile in aqueous sodium acetate. The yellow precipitate was washed with water and recrystallized from methanol. It melted at 177°C with decomposition.

Because CCCP is hydrolyzed in aqueous solutions fairly rapidly (we found a 10^{-5} M solution was approximately 50% decomposed in one day at pH 7), it was essential that these solutions be prepared immediately before use.

The aqueous solutions contained: 0.1 M NaCl (to establish a large excess of indifferent electrolyte and to supply Cl^- ions to enable use of Ag/AgCl electrodes); 0.05 M phthalate-phosphate-borate buffers to the desired pH; and the desired concentration of CCCP, obtained by adding 1 ml of a concentrated solution of CCCP in 95% ethanol to a 100-ml flask already containing the NaCl and buffer, and diluting to volume. The alcohol solutions were used rather than directly dissolving the CCCP in water because the latter process is very slow. The alcohol solutions were invariably prepared within two days, and the aqueous solutions within 1 hr of actual measurement in the bilayer apparatus.

The lipid solution for forming the bilayer membranes consisted of an equimolar mixture of egg lecithin (Pangborn, 1951) and cholesterol dissolved to 19% by weight in *n*-decane.¹ Several lipid solutions using three different batches of egg lecithin gave identical results. We prefer these fairly concentrated lipid solutions rather than the 1 to 2% solutions more commonly used, because they give bilayers of longer life and more stable electrical properties. No doubt the conductivity, in particular, must be a function of the composition of the membrane-forming lipid solution, but we have not explored this question in detail, preferring to keep this variable fixed for the present purposes.

The procedure for bilayer formation and the Teflon measuring cell were the same as described previously (LeBlanc, 1969). So also was the electrical apparatus, except that fiber junction-saturated calomel electrodes were used to measure membrane potentials in experiments with concentration gradients. In these experiments, the gradients were established by changing the aqueous solution on one side of the bilayer with an infusion-withdrawal pump. When a pH gradient was used, the pH in the varying solu-

¹ Neither lecithin nor cholesterol individually is this soluble in *n*-decane, but a 1:1 molar mixture is soluble to at least 50% by weight.

tion was continuously monitored with a calibrated glass electrode. When the CCCP concentration was varied, a sample of the final solution was withdrawn and the concentration of CCCP determined spectrophotometrically. Even with vigorous stirring there was always a delay of approximately 1 min before the transmembrane potential attained a steady value. This was probably an expression of the presence of unstirred layers adjacent to the membrane.

Conductivity determinations were always performed with identical aqueous solution on either side of the membrane. Conductivities were obtained by plotting steady state current-voltage characteristics on an X-Y recorder and taking the slope at zero current. Background conductivities, without CCCP, were always of the order of $10^{-7} \Omega^{-1} \text{ cm}^{-2}$. These were subtracted from the values obtained in the presence of CCCP to obtain the reported figure, supposedly characteristic of CCCP itself. This is admittedly a debatable procedure, and we arbitrarily decided to use only those data where this correction was 20% or less. This established a lower limit to the CCCP concentration that could be used.²

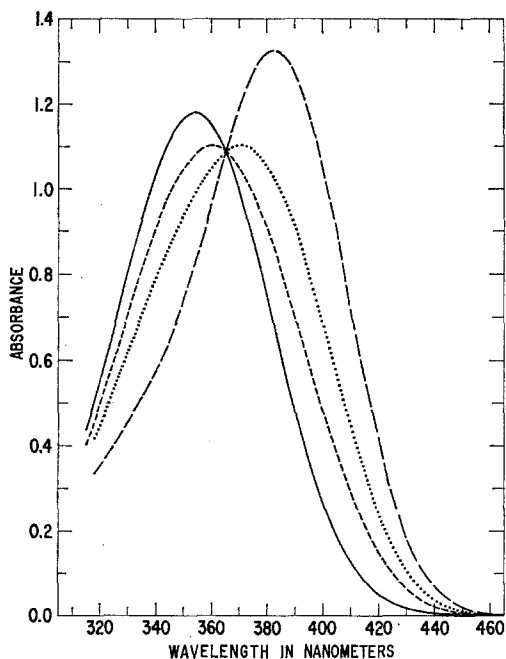


Fig. 1. Spectrophotometric determination of pK_a for CCCP. The aqueous solutions contained $5.19 \times 10^{-5} \text{ M}$ CCCP, 0.1 M NaCl, 1% ethanol, and 0.05 M buffer to pH: ——— 3.0, - - - 9.0, - - - - 5.68 \pm 0.01, ······ 6.15 \pm 0.01. Spectra were taken with a Cary model 14 recording spectrophotometer. The spectra at pH 3.0 and 9.0 were taken as representative of undissociated and dissociated acid, respectively. The isobestic point is at 365 nm. Values of K_a were calculated from absorbances at 340, 350, 380, 390, 400, and 410 nm for each intermediate pH, yielding $K_a = 8.0 \pm 0.2 \times 10^{-7}$ and $8.2 \pm 0.2 \times 10^{-7}$ mole/liter for pH = 5.68 and 6.15, respectively. The mean is $K_a = 8.1 \pm 0.3 \times 10^{-7}$ mole/liter, or $pK_a = 6.09 \pm 0.02$. $T = 26^\circ \text{ C}$

2 The background conductance obtained with the lipid composition used here is invariably one order of magnitude or more higher than we, and others, can obtain with other membrane-forming solutions. We feel the greater stability and reproducibility of the background value with the present membranes outweigh this disadvantage.

Determination of pK_a

Heytler (1963) reported a value of 5.95 for the pK_a of CCCP, without specifying the exact procedure. In order to analyze our data, we need the value of pK_a in the same solutions used for the bilayer measurements, i.e., at the same ionic strength, etc. Therefore, pK_a was determined spectroscopically, as illustrated in Fig. 1, with aqueous solutions prepared as described above. The pK_a value obtained of 6.09 ± 0.02 is about 2% higher than reported by Heytler.

Results

Conductivity Data for CCCP

Fig. 2 illustrates the dependence of conductivity upon aqueous uncoupler concentration at several values of pH. For lower concentrations, at each pH the conductivity is directly proportional to concentration.

For higher concentrations, the conductivity is independent of concentration. Examination of the several curves in Fig. 2 shows that the departure from linearity is determined by the conductivity level rather than by the concentration; i.e., there is a maximum conductivity of 3 to $6 \times 10^{-5} \Omega^{-1} \text{ cm}^{-2}$ which is only weakly pH-dependent. The appearance with CCCP of a maximum conductivity is reminiscent of that found with tetraphenylborate (LeBlanc, 1969), which we attributed to the onset of space-charge-limited currents. The same phenomenon is also found with carbonylcyanide 2,4,5-trichlorophenylhydrazone (Lieberman & Topaly, 1968*b*).

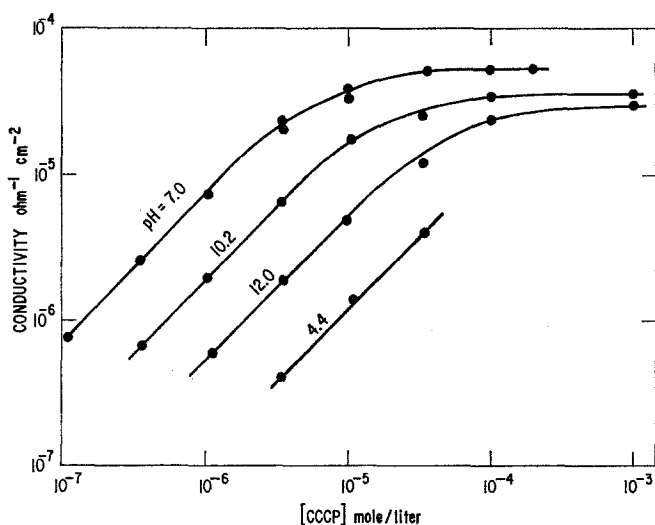


Fig. 2. Dependence of conductivity upon CCCP concentration at several values of pH. The curves here are not theoretical. The conductivity is directly proportional to concentration at lower concentrations for each pH. The highest concentrations used at pH 4.4 and 7.0 were just below the saturation values. $T=26^\circ \text{C}$

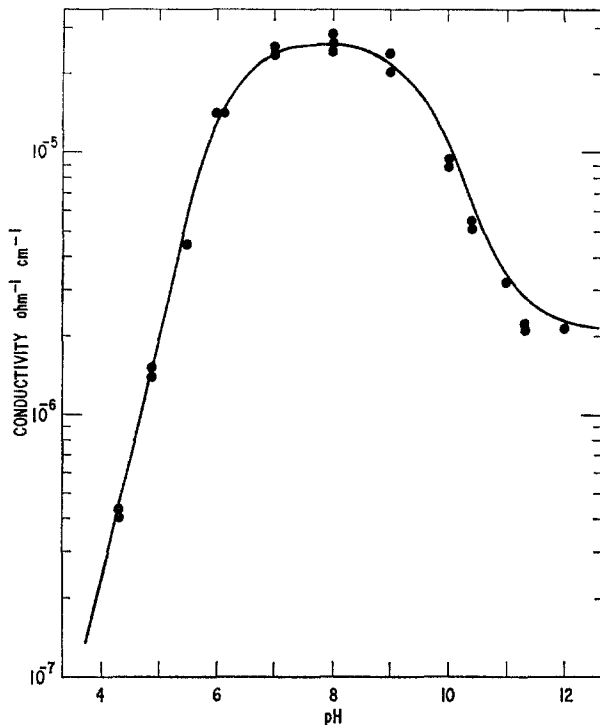


Fig. 3. Dependence of conductivity upon pH at a fixed CCCP concentration of 3.46×10^{-6} M. The theoretical curve is from Eq. (10), using the values 3.6×10^{-4} , 2.0×10^{-3} , and 11 cm/sec for D_A/δ , P_A , and P_{HA} . $T=26^\circ\text{C}$

Whatever the cause of the concentration-independent conductivities, no theory exists that gives a quantitative analysis of the data in this region. The model developed later in this paper, for example, is clearly inapplicable there. Therefore, in comparing the model with experiment, we are constrained to choose conductivity data at lower concentrations, in the range where conductivity is dependent upon concentration.

Fig. 3 shows the dependence of conductivity upon pH at a fixed CCCP concentration of 3.46×10^{-6} M, where the conductivity is essentially linear with CCCP concentration at all pH values. There is a maximum in the conductivity in the neighborhood of pH 8, i.e., approximately two pH units to the alkaline side of the $\text{p}K_a$ of CCCP. At low pH, the conductivity varies inversely with $[\text{H}^+]$. On the alkaline side of the maximum, the pH dependence is more complicated. As pH increases, the conductivity first decreases and then becomes essentially constant beyond pH 11.

The current-voltage characteristics at $\text{pH} \lesssim 10$ were always mildly super-linear and exhibited no time delays other than those owing to the resistance-

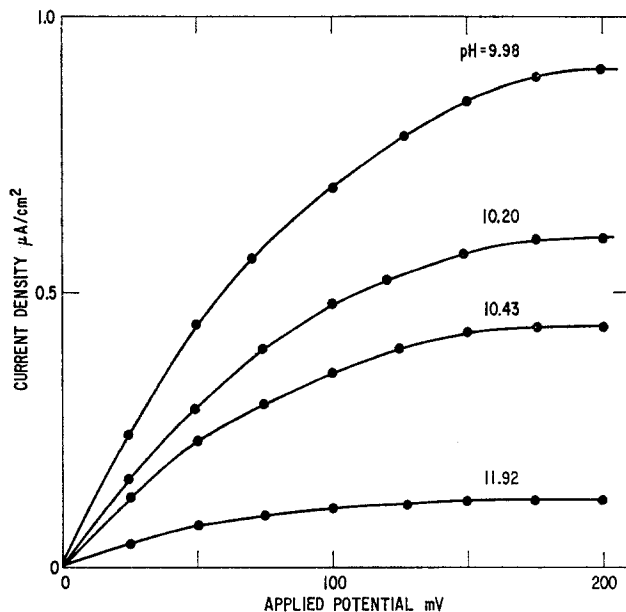


Fig. 4. Current-voltage characteristics with a CCCP concentration of 3.46×10^{-6} M at high pH. The curves here are not theoretical. $T = 26^\circ\text{C}$

capacitance time constants of the system. At $\text{pH} \geq 10$, there was a noticeable time delay after the potential was set before the current settled to its steady state value. This time delay increased with increasing pH, reaching a value of several tens of seconds at pH 12. Furthermore, the steady state current-voltage characteristics all saturated beyond pH 10, as illustrated in Fig. 4.

These phenomena at high pH presented the clue to the interpretation of all our results. The long time delays and the saturating current-voltage characteristics are again reminiscent of the behavior observed with tetraphenylborate (LeBlanc, 1969) and are undoubtedly here, as they are there, associated with concentration polarization in unstirred aqueous layers adjacent to the membrane.

Fig. 5 shows that the saturation current, measured from curves such as those in Fig. 4, varies linearly with $[\text{H}^+]$. This result is predicted by the model described later.

One may wonder at this point why current saturation is not found at lower pH values. Fig. 4 shows (and the model also predicts) that the saturation current increases with $[\text{H}^+]$ more rapidly than does the conductivity (initial slope of the current-voltage characteristic). Hence, the voltage at which saturation occurs also increases with $[\text{H}^+]$. For $\text{pH} \lesssim 10$, this voltage

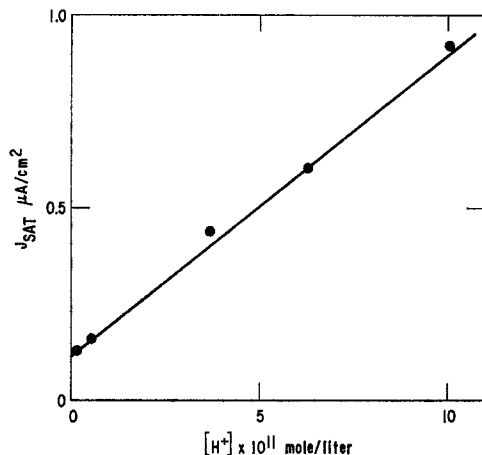


Fig. 5. Saturation current density vs. $[H^+]$ at a CCCP concentration of 3.46×10^{-6} M. Eq. (12) gives the theoretical curve shown with values 3.6×10^{-4} and 9.8 cm/sec for D_A/δ and P_{HA} . $T=26^\circ C$

becomes greater than 200 mV, which is the level at which the membranes almost invariably undergo electrical breakdown. Thus, for $pH \lesssim 10$, measurements cannot be made at voltages high enough to observe saturation.

Membrane Potential Data for CCCP

Membrane potentials at zero current were measured both with pH gradients but the same total CCCP concentration on each side of the membrane, and with CCCP concentration gradients with the same pH on each side.

In the pH-gradient experiments, the pH of the exchanged solution could be measured continuously, so it is possible to present the results in the most convenient form of the derivative of potential with pH gradient at zero gradient. These data are shown in Fig. 6. For pH values between 6 and 9, the bilayer acts as a perfect H^+ electrode, within experimental error, giving the Nernstian value of 59.4 mV/unit pH gradient. At higher and lower pH, the potentials fall off toward zero.

The experiments with CCCP concentration gradients were more tedious experimentally and are more difficult to present in the form of a graph. Since the final CCCP concentration of the exchanged solution could be determined only at the termination of an experiment by withdrawing a sample for analysis, the experiments had to be performed one at a time, and the value of the CCCP concentration gradient varied from one experi-

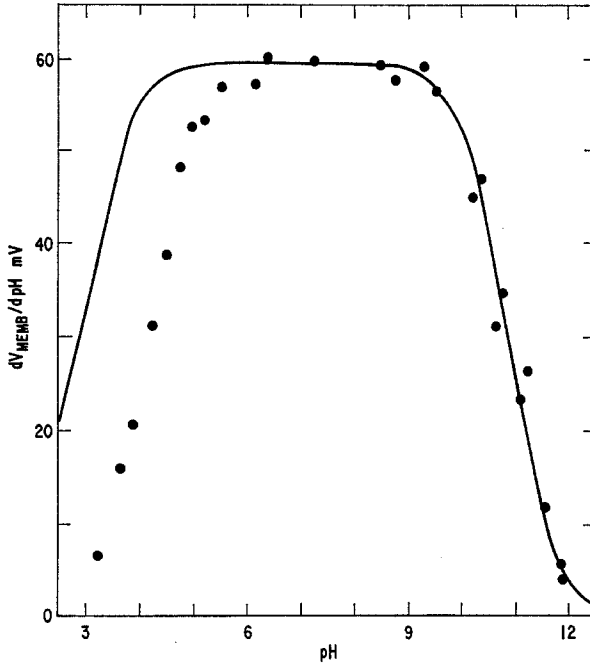


Fig. 6. Membrane potentials induced by pH gradients for a CCCP concentration of 3.46×10^{-5} M on each side of the membrane. The derivative of potential with pH gradient at zero gradient is plotted. The curve at high pH is calculated from Eq. (19) using 3.6×10^{-4} and 11 cm/sec for D_A/δ and P_{HA} . The curve at low pH is calculated from Eq. (22) using 2.0×10^{-3} cm/sec for P_A and a value of $5 \times 10^6 \Omega \text{ cm}^2$ for the leakage resistance. $T=26^\circ \text{C}$

ment to the next. The Table displays the raw data obtained in one sequence of measurements. In order to present these results coherently in graph form, the model described in the following sections was used to calculate a

Table. Membrane potential data with the same pH on either side but with a gradient in CCCP concentration ($T=26^\circ \text{C}$)

pH	[CCCP] _{OUT} (μM)	[CCCP] _{IN} (μM)	$\psi_{\text{OUT}} - \psi_{\text{IN}}$ (mV)	$P_{HA} \delta / D_A^a$ ($\times 10^{-4}$)
10.4	20	3.50	10	2.9
10.8	25	3.46	18	3.0
11.1	23	3.47	22	3.6
11.4	22	3.50	33	2.8
11.6	23	3.47	36	3.4
12.0	25	3.47	45	2.9

^a Values of $P_{HA} \delta / D_A$ calculated from the data using Eq. (20).

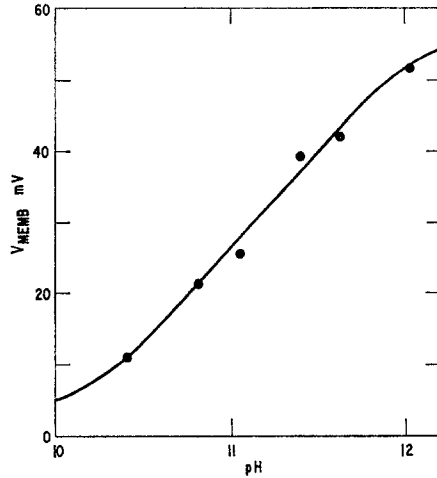


Fig. 7. Membrane potentials induced by 10-fold CCCP concentration gradients with the same pH on each side. The points are calculated from the data of the Table as described in the text. The curve is from Eq. (20), using values of 3.6×10^{-4} and 11 cm/sec for D_A/δ and P_{HA}

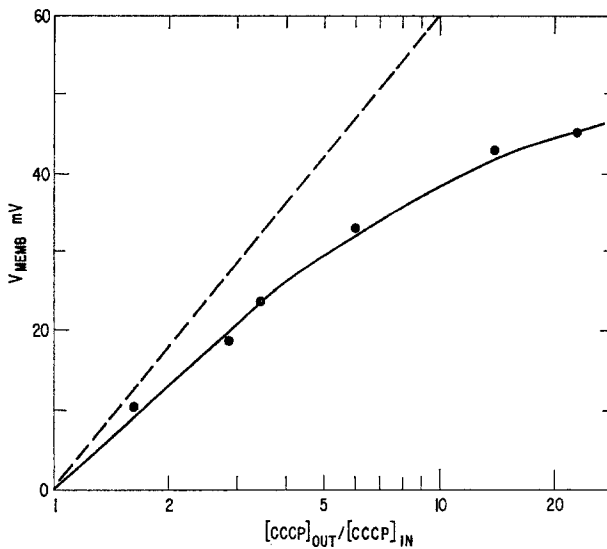


Fig. 8. Membrane potential vs. CCCP concentration ratio at a pH of 11.4 on either side of the membrane. The concentration of CCCP inside was $1.0 \mu\text{M}$. The dotted curve is the Nernst potential (59.4 mV for a 10-fold ratio); the solid curve is calculated from Eq. (20) using 3.6×10^{-4} and 11 cm/sec for D_A/δ and P_{HA} . $T=26^\circ\text{C}$

value for the quantity $\delta P_{HA}/D_A$ for each pH data point; then the model was used again, with this value, to calculate a membrane potential at the pH for a 10:1 CCCP concentration ratio. These calculated potentials still contain the experimental error. They are shown in Fig. 7.

In order to demonstrate the validity of this procedure (and to further test the model, which predicts a rather surprising dependence of potential on uncoupler concentration gradient), we measured potentials over a wide range of CCCP concentration ratios at a fixed pH of 11.4. These raw data are presented in Fig. 8. It is seen that the potential is a highly nonlinear function of concentration ratio, and the data are fit well by the model with a single value of the parameter $\delta P_{HA}/D_A$.

Theoretical Model

A fundamental assumption of this treatment is that the nature of the membrane itself is independent of pH. In particular, we assume that permeability coefficients are pH-independent. That this is only approximately true for the bilayers used in the CCCP experiments is demonstrated by the fact that the maximum conductivities at high CCCP concentrations do exhibit a weak pH dependence (Fig. 2).

We present here a simplified version of the model, which fits the data for CCCP, in which it is assumed that the uncoupler species HA and A^- are in chemical equilibrium with H^+ everywhere in the two aqueous phases:

$$[H^+][A^-]/[HA] = K_a. \quad (1)$$

This cannot be true immediately adjacent to the membrane with non-zero fluxes through the membrane. The reasons why this approximation appears to be valid are discussed in the Appendix, where a more rigorous treatment is given.

We consider only the case of the steady state. We assume that HA and A^- are the only species transported through the membrane. Since A^- is the sole ion transported, the steady state current density, j , as measured by the external circuit current, is related to the flux, J_A^m , of A^- within the body of the membrane, by $j = -eJ_A^m$.

We recognize the existence of unstirred aqueous layers adjacent to the membrane. We assume a sufficiently large excess of indifferent electrolyte such that the electric field can be taken as zero throughout the water. Hence, all species must be transported through the unstirred layers purely by diffusion.

We idealize the structure of the unstirred layers in the usual fashion by assuming that they extend to a sharply defined distance, δ , on each side of the membrane. Beyond these distances, in the bulk water phases, the solutions are assumed to be perfectly mixed. Finally, we assume a sufficiently

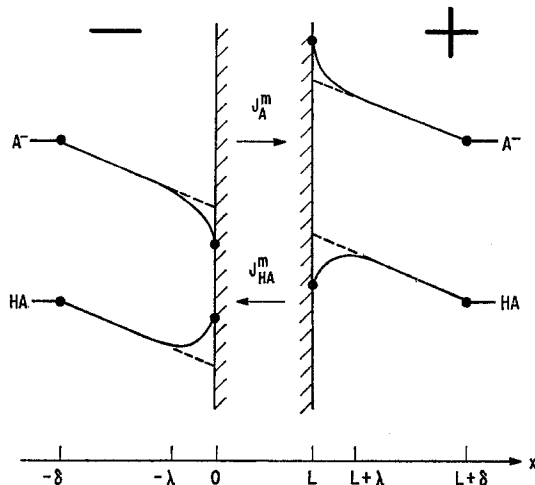


Fig. 9. Schematic diagram showing concentration profiles in the unstirred water layers. Here we imagine the same bulk concentrations on either side of the membrane and an applied potential driving a positive flux of the anion A^- . The thickness of the unstirred layers is δ ; the equilibrium distance is λ (see Eq. (A.14) of the Appendix). In the simplified model of the text, we assume that λ is so much smaller than δ that we may calculate the concentrations of A^- and HA directly at the membrane/water interfaces by extrapolating their gradients at large distances (i.e., by using the dotted lines above where A^- and HA are in chemical equilibrium with H^+). Actually, at distances of the order of λ or less from the interfaces A^- and HA are not generally in equilibrium with H^+ and their concentration profiles are curved such as shown by the solid lines

large excess of buffer that $[H^+]$ can be taken as constant even in the unstirred layers.

Since HA and A^- undergo chemical reaction, their individual fluxes are not necessarily constant, but the sum of their fluxes is constant in the steady state. Hence, the sum of J_{HA}^m , the transmembrane flux of HA, and J_A^m is equal to the sum of the diffusion fluxes of A^- and HA in the unstirred layers:

$$J_A^m + J_{HA}^m = -D_A d[A]/dx - D_{HA} d[HA]/dx \quad (2)$$

where D_A , D_{HA} and $[A]$, $[HA]$ are the respective diffusion constants and concentrations in the water. The variable x is a coordinate normal to the membrane, which is idealized as an infinite slab of thickness L with boundaries at $x=0$ and L (see Fig. 9).

Notice from Eq. (2) that the flux of A^- in the unstirred layers is not necessarily equal to the flux of A^- in the membrane. Thus, A^- does not carry all the electric current in the unstirred layer. The remainder is carried by diffusion of buffer ions.

The values of $[A]$ and $[HA]$ immediately at the membrane/water boundaries, in terms of membrane fluxes and bulk concentrations, can be obtained by integrating Eq. (2) and substituting from Eq. (1). Define the reduced proton concentration as $h_0 \equiv [H^+(0)]/K_a$ and, $h_L \equiv [H^+(L)]/K_a$. The integration yields:

$$[A(0)] - [A]_0 = ([HA(0)] - [HA]_0)/h_0 = -(J_A^m + J_{HA}^m) \delta / (D_A + D_{HA} h_0) \quad (3)$$

and

$$[A(L)] - [A]_L = ([HA(L)] - [HA]_L)/h_L = +(J_A^m + J_{HA}^m) \delta / (D_A + D_{HA} h_L) \quad (4)$$

where $[A]_0$, $[HA]_0$ and $[A]_L$, $[HA]_L$ are the respective bulk concentrations in the two aqueous phases.

The bulk concentrations and the flux J_A^m are experimentally defined quantities (the latter from the current), so the problem is solved if we have one more equation for the unknown flux J_{HA}^m . This is simply:

$$J_{HA}^m/P_{HA} = [HA(0)] - [HA(L)] \quad (5)$$

where P_{HA} is the membrane permeability coefficient of HA. Eq. (5) can be combined with Eqs. (3) and (4) to yield an expression for J_{HA}^m in terms of J_A^m and bulk concentrations.

In order to simplify the algebra in presenting the rest of the model, we specialize the equations to two cases: (1) where the external circuit current, and therefore J_A^m , is not zero but with the various bulk concentrations equal on both sides of the membrane (this corresponds to the experimental situation chosen in the conductivity measurements); and (2) where the external circuit current, and therefore J_A^m , is zero but with different bulk concentrations on either side of the membrane (corresponding to the membrane potential experiments).

Model for Conductivity Experiments

In the first case, the relation for J_{HA}^m is:

$$J_{HA}^m/J_A^m = -2P_{HA} \delta (2P_{HA} \delta + D_{HA} + D_A/h)^{-1}. \quad (6)$$

Substituting into Eqs. (3) and (4), we then obtain expressions for the concentrations $[A(0)]$ and $[A(L)]$ in terms of bulk concentrations $[A]_0 = [A]_L = [A]$ and J_A^m :

$$[A(0)] - [A] = [A] - [A(L)] = -J_A^m [D_A/\delta + h(2P_{HA} + D_{HA}/\delta)]^{-1}. \quad (7)$$

From Eq. (7), we can derive the conductivity, $\sigma_0 \equiv e(dJ_A^m/dV)_{V=0}$, where V is the applied potential, by the following argument. Define the permeability coefficient of A^- , P_A , by:

$$J_A^m/P_A \equiv [A(0)] - [A(L)] \quad (V=0). \quad (8)$$

If the flux J_A^m is related to the gradient in chemical potential of A^- , then, in the presence of a sufficiently small V , we expect:

$$J_A^m/P_A \cong [A(0)] - [A(L)] + [A]eV/kT. \quad (9)$$

This equation is true only if the potential gradient is constant in the membrane (i.e., in the absence of significant space-charge effects), and is thus equivalent to the Goldman approximation.

Substituting for $[A(0)]$ and $[A(L)]$ from Eq. (7), solving for J_A^m , and writing $[A] = [HA]^{tot}/(1+h)$ where $[HA]^{tot}$ is the total uncoupler concentration, we find:

$$\sigma_0 = [HA]^{tot} P_A \frac{e^2}{kT} \frac{(\beta+h)}{(1+h)(\alpha+\beta+h)} \quad (10)$$

where the parameters α and β are defined by:

$$\begin{aligned} \alpha &\equiv 2P_A \delta (2P_{HA} \delta + D_{HA})^{-1} \\ \beta &\equiv D_A (2P_{HA} \delta + D_{HA})^{-1}. \end{aligned} \quad (11)$$

Returning to Eq. (7), we also see that there must be an upper limit to the flux J_A^m where, depending upon its sign, either $[A(0)]$ or $[A(L)]$ vanishes. This condition defines a saturation current density equal to:

$$j_{SAT} = e[HA]^{tot} (1+h)^{-1} [D_A/\delta + h(2P_{HA} + D_{HA}/\delta)]. \quad (12)$$

The saturation current at a given $[HA]^{tot}$ and pH is determined purely by the unstirred layers and by P_{HA} , so that Eq. (12), unlike Eq. (10), is not dependent on the constant field assumption.

The physical significance of these equations is as follows. Suppose, as in Fig. 9, that the applied potential is such as to give a positive J_A^m . Then $[A^-]$ decreases on the left side of the membrane and increases on the right side due to the voltage-driven flux of A^- . This leads to the concentration polarization expressed in Eq. (7). But these changes in $[A^-]$ are partially offset by the reaction $HA = A^- + H^+$ occurring in the water just adjacent to the membrane/water boundaries, which in turn consumes HA on the left side and produces it on the right. Thus, an HA gradient also develops

which tends to drive HA back through the membrane in the opposite sense of J_A^m , hence, the minus sign in Eq. (6).

Furthermore, from Eq. (6) we see that if $2P_{HA}\delta \gg D_{HA} + D_A/h$, then $J_{HA}^m \approx -J_A^m$, or $J_{HA}^m + J_A^m \approx 0$. In this case, the back flux of HA almost completely offsets the forward flux of A. The concentration polarization is nil, as is seen most clearly by referring back to Eqs. (3) and (4); therefore, the saturation current given by Eq. (12) is large.

On the other hand, as $[H^+]$ and therefore h goes to zero, $2P_{HA}\delta \ll D_{HA} + D_A/h$. Then we see from Eq. (6) that $J_{HA}^m \ll J_A^m$ (when $[H^+] \rightarrow 0$ then $[HA]/[A^-] \rightarrow 0$, and the back flux of HA cannot offset the forward flux of A^-). Thus, at high pH, one obtains the full concentration polarization of A^- alone.

We are now in a position to understand why there can be a maximum in the conductivity at a certain pH. The variation of σ_0 as $[H^+]^{-1}$ at low pH is easy to understand: the species A^- is the sole current carrier in the membrane, and its concentration varies inversely with $[H^+]$ for $pH \ll pK_a$. What is not so obvious is why, in this model, with increase in pH up to and beyond pK_a , the conductivity does not increase with $[A^-]$ monotonically to a constant value. Why does the conductivity go back down for $pH \gg pK_a$?

The answer is again related to concentration polarization. The conductivity is determined by the $[A^-]$ concentration at the membrane/water boundaries, or more accurately, by $[A(0)]$ or $[A(L)]$, whichever is smaller. If P_{HA} is sufficiently large so that $P_{HA}\delta \gg D_{HA} + D_A/h$ at h in the neighborhood of one ($pH \approx pK_a$), for example, there is little concentration polarization and the bulk concentration $[A]$ determines the conductivity. For a sufficiently small value of h , ($pH \gg pK_a$) $P_{HA}\delta \ll D_{HA} + D_A/h$, and there can be significant polarization if we also have the condition $P_A > D_A/\delta$, i.e., if the permeability of A^- is faster than its diffusion through the unstirred layers. In this case, the conductivity at high pH is less than that near pK_a where concentration polarization was negligible.³

From Eq. (10), we find that the maximum conductivity occurs for $h = h_{\max}$ where:

$$h_{\max} = -\beta + [\alpha(1-\beta)]^{\frac{1}{2}}. \quad (13)$$

Since this quantity must be real and positive, the conditions $\beta < 1$ and $2\beta < -\alpha + (\alpha^2 + 4\alpha)^{\frac{1}{2}}$ must both be satisfied in order that a maximum occur.

³ The instantaneous conductance, immediately after voltage application and before concentration polarization has developed, should, on the other hand, increase with increasing pH monotonically with the bulk A^- concentration. We have not investigated this point experimentally.

These conditions are an exact statement of the qualitative inequalities discussed in the previous paragraph. If $\beta \ll 1$, $\sqrt{\alpha}$ (which is true for the parameters derived for CCCP), then it follows that:

$$h_{\max} \equiv [\text{H}^+]_{\max}/K_a \approx (P_A/P_{\text{HA}})^{\frac{1}{2}}. \quad (14)$$

Thus the pH at maximum conductivity falls to the alkaline or acid side of $\text{p}K_a$ depending primarily on whether $P_A < P_{\text{HA}}$ or vice versa. In the Discussion, we argue that the permeability coefficient of the ion A^- must almost certainly be orders of magnitude smaller than that of the neutral molecule HA. Hence, the conductivity maximum occurs to the alkaline side of $\text{p}K_a$.

Model for Membrane Potential Experiments

In these experiments, $J_{\text{A}}^m = 0$, but the various bulk concentrations are not equal on either side of the membrane. Here the equation used to eliminate the variable J_{HA}^m is:

$$\frac{J_{\text{HA}}^m}{P_{\text{HA}}} = \frac{h_0 [\text{HA}]_0^{\text{tot}} (1 + h_0)^{-1} - h_L [\text{HA}]_L^{\text{tot}} (1 + h_L)^{-1}}{1 + \delta P_{\text{HA}} [h_0 (D_A + D_{\text{HA}} h_0)^{-1} + h_L (D_A + D_{\text{HA}} h_L)^{-1}]}. \quad (15)$$

Substitution into Eqs. (3) and (4) yields equations for $[\text{A}(0)]$ and $[\text{A}(L)]$ as before. From these concentrations, we can write down immediately the membrane potential, but only if we make the further implicit assumption that the fluxes are small enough that the concentration of A^- at the boundaries just within the membrane is related to the concentration just outside by the equilibrium distribution coefficients. (Even though J_{A}^m is zero, the fluxes of A^- at the two boundaries in the water are not necessarily so, as is hopefully made clear in the Appendix.) Under this assumption we have

$$e[\psi(L) - \psi(0)]/kT = \log [\text{A}(L)]/[\text{A}(0)]. \quad (16)$$

Again to avoid as much as possible writing complicated algebraic equations we specialize to two cases: (1) a pH gradient but the same $[\text{HA}]^{\text{tot}}$ on either side, and (2) an $[\text{HA}]^{\text{tot}}$ gradient but the same pH on either side.

For a pH gradient alone, we find:

$$\psi(L) - \psi(0) = \frac{kT}{e} \log \frac{(1 + h_0) + P_{\text{HA}} \delta h_0 S(h_0, h_L)}{(1 + h_L) + P_{\text{HA}} \delta h_L S(h_0, h_L)} \quad (17)$$

where the quantity

$$S(h_0, h_L) \equiv (1 + h_0)(D_A + D_{\text{HA}} h_0)^{-1} + (1 + h_L)(D_A + D_{\text{HA}} h_L)^{-1} \quad (18)$$

is either $2/D_A$ or $2/D_{HA}$ depending on whether h_0 and h_L are small or large compared to one. Clearly, if the terms in h in Eq. (17) are large compared to one (low pH), the membrane acts as an H^+ electrode, whereas at sufficiently small h_0 and h_L (high pH), the potential vanishes. The membrane potential data we wish to analyze here are in the form $\Delta V/\Delta pH$, in the limit of zero ΔpH . Differentiating Eq. (17) with respect to h_0 or h_L and keeping the other constant, then setting $h_0 = h_L = h$ yields:

$$\frac{d[\psi(L) - \psi(0)]}{d pH} = \frac{kT}{e} \frac{h[1 + \delta P_{HA} S(h, h)]}{1 + h[1 + \delta P_{HA} S(h, h)]} \quad (19)$$

which is kT/e for large h , and zero for small h .

For an $[HA]^{tot}$ gradient alone, $h_L = h_0 = h$, and a similar procedure yields

$$\psi(L) - \psi(0) = \frac{kT}{e} \log \frac{R + P_{HA} \delta h(1 + R)(D_A + D_{HA} h)^{-1}}{1 + P_{HA} \delta h(1 + R)(D_A + D_{HA} h)^{-1}} \quad (20)$$

where $R \equiv [HA]_L^{tot}/[HA]_0^{tot}$. For sufficiently small h , the argument of the logarithm is R , which is just the concentration ratio of A^- itself at high pH; hence the membrane acts as an A^- electrode. For large h (low pH), the potential vanishes.

Thus we see that the membrane is an H^+ electrode at low pH, and an A^- electrode at high pH.

A somewhat surprising result predicted by Eq. (20) is that the membrane potential has an upper limit when the concentration ratio R becomes indefinitely large:

$$\lim_{R \uparrow \infty} [\psi(L) - \psi(0)] e/kT = \log [1 + (D_A + D_{HA} h) \delta P_{HA} h] \quad (21)$$

which is itself indefinitely large only for $h \rightarrow 0$. No such thing happens with pH gradients alone.

Comparison of Model with CCCP Data

The model gives an excellent qualitative description of most of the CCCP data. It predicts correctly a direct dependence of conductivity on CCCP concentration (except at higher concentrations where presumably space-charge effects invalidate the constant-field approximation). It predicts the correct functional dependence of conductivity on pH. It predicts current saturation at high pH and the correct dependence of saturation-current density upon $[H^+]$. It predicts correctly that the membrane acts as an H^+ electrode at low pH, and an A^- electrode at high pH. Finally, it predicts

correctly the rather peculiar dependence of membrane potential on CCCP concentration ratio at high pH.

Furthermore, it is possible quantitatively to fit these data with a self consistent set of parameters.

As illustrated by the Table and Figs. 6, 8 and 9, the various membran potential data at high pH are fit extremely well using a figure of 3×10^4 for the single parameter $P_{HA} \delta/D_A$. Analysis of all these data suggests a probable error of about 20% and a figure of $P_{HA} \delta/D_A = 3.0 \pm 0.6 \times 10^4$.

The saturation current density at $[H^+] = 0$ is D_A/δ according to Eq. (12) and its derivative with $[H^+]$ is $(2P_{HA} + D_{HA}/\delta)/K_a$. The data of Fig. 5 thus analyzed give $D_A/\delta = 3.6 \pm 0.4 \times 10^{-4}$ and $P_{HA} + D_{HA}/2\delta = 9.5 \pm 1.0$ cm/sec. Since D_{HA} must be of approximately the same magnitude as D_A , the latter figure must be P_{HA} itself, so that $P_{HA} \delta/D_A = 2.6 \pm 0.5 \times 10^4$ from these data which compares very well with the value obtained from the potential measurements. The figure for D_A/δ compares with the value of 3.6×10^{-4} cm/sec found for tetraphenylborate using the same cell (LeBlanc, 1969). The thickness of the unstirred layers, δ , is most probably determined by the geometrical thickness of the Teflon septum. This is about 10^{-2} cm, close to the value of δ determined directly in the tetraphenylborate experiments. Hence, the aqueous diffusion constant of the CCCP anion must be close to that of tetraphenylborate, i.e., 5×10^{-6} cm²/sec, as is reasonable.

The value of P_A , the permeability coefficient of the CCCP anion, is best obtained from the conductivity at low pH, where it varies inversely with $[H^+]$, using Eq. (10). The value obtained is $2.0 \pm 0.2 \times 10^{-3}$ cm/sec. This parameter could also be determined from the current-voltage characteristic at high pH, but because $P_A \gg D_A/\delta$, that procedure does not yield an accurate value (LeBlanc, 1969). We note again, however, that the appearance of current saturation at high pH is consistent with this large P_A figure obtained at low pH.

Finally, the three parameters P_{HA} , P_A , and D_A/δ now fixed equal to 11 ± 2 , $2.0 \pm 0.2 \times 10^{-3}$, and $3.6 \pm 0.4 \times 10^{-4}$ cm/sec, respectively, permit the calculation from Eq. (10) of the full pH-dependent conductivity as shown in Fig. 3. The fit to the data is excellent. The maximum conductivity is predicted to occur at a pH of 7.96, i.e., approximately two pH units to the alkaline side of pK_a , in agreement with the observations.

The one phenomenon we are unable to account for in a fully satisfactory manner is the fall in the H^+ -gradient-induced membrane potential at low pH (Fig. 6). This is undoubtedly connected with the fall in conductivity at low pH (Fig. 3) and the presence of a non-zero background conductivity. But using the Goldman constant-field approximation and the

equations derived here, we find at low pH:

$$d[\psi(L) - \psi(0)]/d \text{pH} \cong (kT/e) \sigma_0 (\sigma_0 + \sigma_{\text{leak}})^{-1} \quad (22)$$

where σ_0 is given by Eq. (10) and σ_{leak} is the background or "leakage" conductivity. Estimating σ_{leak} as the observed apparent conductivity in the pH 4 range without CCCP present ($2 \times 10^{-7} \Omega^{-1} \text{cm}^{-2}$), we calculate the curve shown in Fig. 6 at low pH. The observed fall in membrane potential occurs approximately one pH unit higher than predicted. The same kind of discrepancy between membrane potential and conductivity data was noted by Markin *et al.* (1969*b*) for the uncoupler tetrachloro-2-trifluorobenzimidazole. Either we are seriously underestimating σ_{leak} or the Goldman equation is being misapplied to our case. Perhaps space-charge effects are the cause of the latter, even though the conductivity is perfectly linear with CCCP concentration at the concentration used and in the neighborhood of pH 4.

Discussion

The three parameters used to fit the CCCP data are D_A/δ , P_A , and P_{HA} , and the values obtained are 3.6×10^{-4} , 2.0×10^{-3} , and 11 cm/sec. The first figure is nominal. The second is comparable to the permeability of the tetraphenylborate anion in similar membranes (LeBlanc, 1969) and probably to that of the phenyldicarbaundecaborane anion, whose flux is also limited primarily by unstirred layers (Lieberman & Topaly, 1969). There are no experimental data with which to compare the value for the third parameter, P_{HA} , and one could hardly hope to find any.

No attempt to measure a permeability as high as 11 cm/sec using direct molecular flux experiments could succeed. With a permeability some four orders of magnitude higher than molecular diffusion velocities through unstirred aqueous layers, the flux would be determined by the unstirred layers to approximately one part in 10^4 , well beyond attainable experimental accuracies.

But our large value for P_{HA} is not unreasonable. From electrostatic considerations, one would expect the neutral species HA to be orders of magnitude more permeable than the charge species A^- through the low dielectric constant bilayer (e.g., Finkelstein, 1970). This expectation is consistent with the observations of Bean, Shepherd and Chan (1968). They measured zero-current isotopic fluxes of several less permeable acids and bases through bilayer membranes. The pH dependence they found was

what one expect if, in each case, the neutral molecules were orders of magnitude more permeable than the respective ionic form.

Thus, our value of 5.5×10^3 for the ratio P_{HA}/P_A is not surprising. What is remarkable about CCCP is that its anion permeability, P_A , is so large. Its high anion permeability is, of course, what makes CCCP such an efficient "proton carrier" in bilayers and, perhaps, such an efficient uncoupler of oxidative phosphorylation.

The present model is, of course, not restricted to uncoupling agents alone. By changing some symbols, it is readily generalized to any system involving a carrier for a nonpermeable ion where there is one-to-one stoichiometry in the ion-carrier complex, and as long as either the carrier or the ion-carrier complex is uncharged. Whichever of these species is uncharged should have the much higher permeability. The mathematics are more complex unless the carried ion is buffered, but in most experiments this can be practically achieved by having the carried ion present in the water in large excess.

These conditions are met by some but not all conductance-inducing agents; for a recent summary, see Mueller and Rudin (1969). For example they are not met by the gramacidins or nystatin, where the stoichiometry is not one-to-one, but they are met by the *n*-actins and valinomycin. For these latter, as for the uncouplers, we submit that, in order to analyze properly the experimental data, it may be necessary to take into account unstirred layers and the expected large permeabilities of the uncharged carriers.

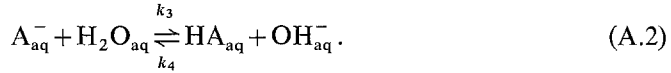
I am greatly indebted to Dr. George M. J. Slusarczuk who kindly prepared the sample of carbonyl cyanide *m*-chlorophenylhydrazone.

Appendix

The simple model of the text assumes that HA, A^- , and H^+ are in chemical equilibrium throughout the water phases. This cannot be true, in general, in the immediate vicinity of the membrane/water interfaces. Yet the simple model is adequate to describe all our experimental data for CCCP, which raises the question: what values of rate constants for various equilibration reactions must be obtained in order that the simple equilibrium model be a good approximation?

We attempt to answer this question with the extended kinetic treatment given here. This extended treatment involves many more parameters than could ever be determined by experiment. It also involves complicated algebraic expressions. For these reasons we ultimately confine our attention to predicting the outcome of the one experiment (the dependence of saturation current density on $[H^+]$ at high pH) where by comparing predictions with CCCP data we can unambiguously say something about the relative magnitudes of various rate constants for the CCCP system.

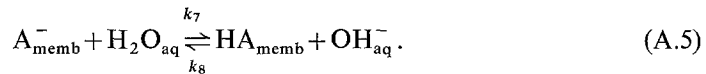
Equilibration can occur through homogeneous reactions in the water phases:



If K_a and K_w are the dissociation constants of HA and water, then:

$$k_2/k_1 = K_w, k_4/k_3 = K_a. \quad (\text{A.3})$$

Equilibration can also occur through heterogeneous reactions at the membrane/water interfaces:



We assume that the activities of OH^- , H^+ , and H_2O inside the membrane are so low that there are no intramembrane homogeneous reactions analogous to (A.1) and (A.2). We also neglect reactions involving buffer species because we imagine they are slower than the corresponding protolytic reactions.

Let $[A_m(x)]$ and $[HA_m(x)]$ represent the concentrations of A^- and HA within the membrane at position x . Let $J_A^w(x)$ and $J_{HA}^w(x)$ be the steady state fluxes in the water phases at x . Because of reactions (A.4) and (A.5), the fluxes of A^- and HA are discontinuous at the two membrane/water interfaces. At $x=L$:

$$\begin{aligned} J_A^m - J_A^w(L) &= -J_{HA}^m + J_{HA}^w(L) \\ &= [A_m(L)](k_5[H^+]_L + k_7) - [HA_m(L)](k_6 + K_w k_8/[H^+]_L). \end{aligned} \quad (\text{A.6})$$

The fluxes in the water at the interfaces are assumed to be linearly related to concentrations. At $x=L$:

$$J_A^w(L) = k_{mw}^A [A_m(L)] - k_{wm}^A [A(L)], \quad (\text{A.7})$$

$$J_{HA}^w(L) = k_{mw}^{HA} [HA_m(L)] - k_{wm}^{HA} [HA(L)]. \quad (\text{A.8})$$

There are equations analogous to (A.6)–(A.8) for $x=0$ in which L is replaced everywhere by zero and the signs of all coefficients on the right-hand sides are reversed. By detailed balancing, we have the relations:

$$k_6/k_5 = K_w, k_8/k_7 = K_a, k_{wm}^A k_{mw}^{HA} / k_{mw}^A k_{wm}^{HA}. \quad (\text{A.9})$$

Consider first the situation in the unstirred layers, where the homogeneous reactions (A.1) and (A.2) occur. At the steady state, both $d[A]/dt$ and $d[HA]/dt$ vanish, so we have the following pair of differential equations:

$$D_A d^2[A]/dx^2 = [A](k_1[H^+] + k_3) - [HA](k_2 + k_4 K_w/[H^+]), \quad (\text{A.10})$$

$$D_{HA} d^2[HA]/dx^2 = -D_A d^2[A]/dx^2. \quad (\text{A.11})$$

Because we assume sufficient excess buffer so that $[H^+]$ is constant, these are equation with constant coefficients and readily solved:

$$[A] = \gamma_1 \exp(x/\lambda) + \gamma_2 \exp(-x/\lambda) + \gamma_3 x + \gamma_4, \quad (\text{A.12})$$

$$[HA] = -[\gamma_1 \exp(x/\lambda) + \gamma_2 \exp(-x/\lambda)] D_A/D_{HA} + [\gamma_3 x + \gamma_4] h \quad (\text{A.13})$$

where the γ 's are constants to be determined by boundary conditions. The quantity λ is the equilibration distance and is defined by:

$$\lambda^{-2} \equiv (k_2 + k_3/h)(D_A + D_{HA} h)/D_A D_{HA}. \quad (\text{A.14})$$

The quantity $h \equiv [H^+]/K_a$, as before. We have made use of relations (A.3) to eliminate k_1 and k_4 .

The boundary conditions at the membrane/water interfaces at $x=0$ and L are:

$$J_A^w(i) = -D_A(d[A]/dx)_i; \quad J_{HA}^w(i) = -D_{HA}(d[HA]/dx)_i \quad (\text{A.15})$$

where $i=0, L$. The boundary conditions at the unstirred layer-bulk solution interface at $x = -\delta$ and $L + \delta$, on the other hand, are written in terms of bulk concentrations

$$[A(-\delta)] = [A]_0; \quad [HA(-\delta)] = [HA]_0, \quad (\text{A.16})$$

$$[A(L+\delta)] = [A]_L; \quad [HA(L+\delta)] = [HA]_L. \quad (\text{A.17})$$

To be consistent, the constant γ_1 in Eqs. (A.12) and (A.13) must be set equal to zero for x positive, and γ_2 must be set equal to zero for x negative.

The fitting of boundary conditions (A.16) and (A.17) is simplified by the knowledge that the equilibration distance λ is much smaller than the thickness δ of the unstirred layers. The following estimates give some idea of the magnitude of λ . We imagine that the second-order rate processes described by k_1 and k_4 are diffusion limited; thus $k_1 \approx k_4 \approx 10^{10}$ mole $^{-1}$ sec $^{-1}$ (Eigen, Kruse, Maass & DeMaeyer, 1964). Since $K_w \approx 10^{-14}$ (mole/liter) 2 and $K_a \approx 10^{-6}$ mole/liter for CCCP, we have $k_2 \approx 10^4$ sec $^{-1}$ and $k_3 \approx 10^2$ sec $^{-1}$ by (A.3). Finally, we estimate $D_{HA} \approx D_A \approx 5 \times 10^{-6}$ cm 2 /sec. With these figures, we see from (A.14) that λ has a maximum value of 2×10^{-5} cm at pH 7. It decreases symmetrically as pH is raised or lowered from 7: $\lambda \approx 2 \times 10^{-6}$ cm at pH 4 and 10, and $\lambda \approx 2 \times 10^{-7}$ cm at pH 2 and 12. Thus, $\lambda \ll \delta \approx 10^{-2}$ cm at all pH values, so that the remaining exponential terms in (A.12) and (A.13) can be neglected in fitting the boundary conditions (A.15) and (A.16) at $x = \delta$ and $L + \delta$.

The solution for $L \leq x \leq L + \delta$ is:

$$[A(x)] = [A]_L + C_{1L} \exp(L-x)/\lambda_L + C_{2L}(L+\delta-x), \quad (\text{A.18})$$

$$[HA(x)] = [HA]_L - (C_{1L} D_A/D_{HA}) \exp(L-x)/\lambda_L + h_L C_{2L}(L+\delta-x) \quad (\text{A.19})$$

where λ_L is defined by (A.14) with $h = h_L$, and

$$C_{1L} \equiv \lambda_L (D_A + D_{HA} h_L)^{-1} [J_A^w(L) D_{HA} h_L/D_A - J_A^w(L)], \quad (\text{A.20})$$

$$C_{2L} \equiv (D_A + D_{HA} h_L)^{-1} [J_A^w(L) + J_{HA}^w(L)]. \quad (\text{A.21})$$

The solution for $-\delta \leq x \leq 0$ is:

$$[A(x)] = [A]_0 + C_{10} \exp x/\lambda_0 + C_{20}(x+\delta), \quad (\text{A.22})$$

$$[HA(x)] = [HA]_0 - (C_{10} D_A/D_{HA}) \exp x/\lambda_0 + h_0 C_{20}(x+\delta) \quad (\text{A.23})$$

where λ_0 is given by (A.14) with $h=h_0$, and C_{10} and C_{20} are defined as in (A.20) and (A.21) except that L is replaced by zero everywhere and the signs are reversed.

The general form of these solutions is sketched as the solid lines in Fig. 9. Since $J_A^w(x) + J_{HA}^w(x) = J_A^m + J_{HA}^m$ for all x , Eqs. (A.18)–(A.23) reduce to Eqs. (3) and (4) of the text when $x-L \gg \lambda_L$ and $x \ll -\lambda_0$; i.e., A^- and HA are essentially in chemical equilibrium with H^+ at distances greater than λ from the membrane/water interfaces. Thus, in the simple model of the text, we are assuming we can accurately approximate the aqueous concentrations of A^- and HA directly at the membrane/water interfaces by ignoring the exponential terms in (A.18), (A.19), (A.22) and (A. 23).

Eqs. (A.18)–(A.23) fix the aqueous concentrations of A^- and HA in the unstirred layers in terms of bulk concentrations, which are observable quantities, and the fluxes $J_A^w(0)$, etc., which are not. To eliminate these latter quantities, we must now consider the heterogeneous reactions (A.4) and (A.5). Using Eqs. (A.6)–(A.9) and (A.18)–(A.23), we find ($i=0$ or L):

$$J_A^w(i)(1 + F_i + G_i h_i) = J_A^m(1 + F_i) + J_{HA}^m F_i, \tag{A.24}$$

$$J_{HA}^w(i)(1 + F_i + G_i h_i) = J_A^m G_i h_i + J_{HA}^m(1 + G_i h_i) \tag{A.25}$$

where the quantities F_i and G_i are defined by

$$\begin{aligned} F_i &\equiv \kappa_i(\lambda_i/D_{HA} + 1/k_{wm}^{HA}) \\ G_i &\equiv \kappa_i(\lambda_i/D_A + 1/k_{wm}^A) \end{aligned} \tag{A.26}$$

and

$$\kappa_i \equiv k_7 k_{wm}^A / k_{mw}^A h_i + k_6 k_{wm}^{HA} / k_{mw}^{HA}. \tag{A.27}$$

Eqs. (A.24) and (A.25) are substituted into (A.18) and (A.19) to yield the following expressions for $[A(L)]$ and $[HA(L)]$ in terms of bulk concentrations and the fluxes J_A^m and J_{HA}^m

$$\begin{aligned} ([A(L)] - [A]_L)(D_A + D_{HA} h_L) &= J_A^m \left[\delta + \lambda_L \frac{(1 + F_L) h_L D_{HA}/D_A - G_L h_L}{(1 + F_L + G_L h_L)} \right] \\ &+ J_{HA}^m \left[\delta + \lambda_L \frac{F_L h_L D_{HA}/D_A - (1 + G_L h_L)}{(1 + F_L + G_L h_L)} \right] \end{aligned} \tag{A.27}$$

and

$$\begin{aligned} ([HA(L)] - [A]_L)(D_A + D_{HA} h_L) &= h_L J_A^m \left[\delta - \lambda_L \frac{1 + F_L - G_L D_A/D_{HA}}{(1 + F_L + G_L h_L)} \right] \\ &+ h_L J_{HA}^m \left[\delta - \lambda_L \frac{F_L - (h_L^{-1} + G_L) D_A/D_{HA}}{(1 + F_L + G_L h_L)} \right]. \end{aligned} \tag{A.28}$$

These are an analogous pair of equations obtained at $x=0$ with L replaced by zero everywhere and all signs reversed on the right-hand sides. The mathematical problem is completed by eliminating J_{HA}^m , the sole remaining unobservable, using (A.28) and its analog at $x=0$ together with Eq. (5) of the text.

Except for the terms in λ_L , Eqs. (A.27) and (A.28) are identical to Eq. (4) of the text. Hence, the simple model described there is clearly a good approximation if all the λ terms are negligible compared to the respective δ terms. From our estimates of the magnitude of λ for CCCP, it follows that in the pH range 3 to 12 all the λ terms are indeed negligible, irrespective of whether F and G are large or small, except the one term

containing h^{-1} in the coefficient of J_{HA}^m in (A.28). This can be large at high pH (low h if F and G are small. For example, at pH 12 ($h \approx 10^{-6}$ for CCCP), we estimate $\lambda \approx 2 \times 10^{-7}$ cm, so $h^{-1} \lambda \approx 10^{-1}$ cm, which is actually one order of magnitude large than δ .

But if this one term in λ is not negligible, we do not predict correctly at least one experimental observation for CCCP, the dependence of saturation current on $[H^+]$. This is shown as follows. Take the bulk concentrations to be equal in the two aqueous phases. Ignore all λ terms in (A.27) and (A.28) except the one containing h^{-1} , and take $F = G = 0$ for the moment. Use (A.28) and its analog at $x = 0$ together with Eq. (5) of the text to find J_{HA}^m as a function of J_A^m and bulk concentrations. Substitute into (A.27) to get $[A(L)]$, and use (A.7) to find $[A_m(L)]$. The condition for current saturation is $[A_m(L)] = 0$ (for negative J_A^m) which yields:

$$j_{SAT}/e[A] = (\delta/D_A + 1/k_{wm}^A)^{-1} + h(1/2P_{HA} + \lambda/D_{HA})^{-1}. \quad (A.29)$$

Eq. (A.29) differs from Eq. (12) of the text in two trivial ways and one nontrivial way. A term in k_{wm}^A is present here and not there because there we assumed $[A_m(L)] \propto [A(L)]$; here we used Eq. (A.7). But the term in k_{wm}^A is negligible for the CCCP system as evidenced by the fact that we must have $P_A \gg D_A/\delta$ in order to see current saturation. Remembering that the definition of the permeability coefficient, P_n , of species n requires that

$$P_n < k_{wm}^n/2. \quad (A.30)$$

We see that $\delta/D_A \gg 1/k_{wm}^A$ for the CCCP system. Also, a term hD_{HA}/δ appears in Eq. (12) and not in Eq. (A.29). This is because we have systematically ignored hD_{HA} with respect to D_A in deriving (A.29) ($h \ll 1$ at the pH values of interest).

The nontrivial new term in (A.29) is the quantity λ/D_{HA} in the coefficient of h . But this term leads to incorrect predictions. The coefficient of h found experimentally for the CCCP saturation current densities at pH 10 to 12 was approximately 20 cm/sec. Therefore, from (A.29), we have $1/2P_{HA} + \lambda/D_{HA} = 0.05$ sec/cm. But we estimate $\lambda \approx 2 \times 10^{-6}$ cm at pH 10, and since $D_{HA} \approx 5 \times 10^{-6}$ cm²/sec, $\lambda/D_{HA} \approx 0.4$ sec/cm at pH 10. Hence Eq. (A.29) cannot fit the experimental data with positive P_{HA} !

Therefore either our estimates of λ are too high by at least an order of magnitude or we cannot ignore the quantities F and G in Eqs. (A.27) and (A.28). We believe the latter is more likely; i.e., the heterogeneous reactions (A.4) and (A.5) must occur with significant rates in the CCCP system.

An estimate of the magnitudes of these rates can be obtained by inquiring how large the quantities F and G must be to reduce the h^{-1} term in (A.28)—and therefore the λ term in (A.29)—to negligible size. We require either F or Gh to be large compared with $\lambda/\delta h$. From the definitions (A.26) and (A.27), we see that at small h there is an h^{-1} term in F which dominates all other terms in F or Gh . Furthermore, using our experimental value of $P_{HA} = 11$ cm/sec and inequality (A.30), we see that $1/k_{wm}^{HA} < 5 \times 10^{-2}$ sec/cm and can probably be ignored with respect to λ/D_{HA} (which we estimate as 4×10^{-2} sec/cm at pH 12, 4×10^{-1} sec/cm at pH 10) in Eq. (A.26) for F . Thus $F \gtrsim \lambda k^7 k_{wm}^A / k_{mw}^A h D_{HA}$, and a sufficient condition for Eq. (12) rather than Eq. (A.29) to be valid is that $k^7 k_{wm}^A / k_{mw}^A \gg D_A/\delta$. But, as we have argued above, $k_{mw}^A \gg D_A/\delta$ for the CCCP system, so we require only that $k^7 \gtrsim k_{mw}^A$ in order that the simple model of the text be valid.

This means that the heterogeneous reactions (A.4) and (A.5) must occur for the CCCP system at rates comparable to those at which A^- and HA are exchanged between membrane and water.

References

- Babakov, A. V., Demin, V. V., Sokolov, S. D., Sotnikov, P. S. 1968. Effect of metal ions on the conductivity and current-voltage characteristics of bimolecular membranes with tetrachlorotrifluorobenzimidazole. *Biofizika* **13**:1122.
- Bean, R. C., Shepherd, W. C., Chan, H. 1968. Permeability of lipid bilayer membranes to organic solutes. *J. Gen. Physiol.* **52**:495.
- Bielawski, J., Thompson, T. E., Lehninger, A. L. 1966. The effect of 2,4-dinitrophenol on the electrical resistance of phospholipid bilayer membranes. *Biochem. Biophys. Res. Commun.* **24**:948.
- Eigen, M., Kruse, W., Maase, G., DeMaeyer, L. 1964. Rate constants of protolytic reactions in aqueous solution. *In: Progress in Reaction Kinetics*, vol. 2. G. Porter, editor. p. 285. MacMillan, New York.
- Finkelstein, A. 1970. Weak-acid uncouplers of oxidative phosphorylation. Mechanism of action on thin lipid membranes. *Biochim. Biophys. Acta* **205**:1.
- Heytler, P. G. 1963. Uncoupling of oxidative phosphorylation by carbonyl cyanide hydrazones. I. Some characteristics of *m*-Cl-CCP action on mitochondria and chloroplasts. *Biochemistry* **2**:357.
- Pritchard, W. W. 1962. A new class of uncoupling agents—carbonyl cyanide phenylhydrazones. *Biochem. Biophys. Res. Commun.* **7**:272.
- Hopfer, U., Lehninger, A. L., Thompson, T. E. 1968. Protonic conductance across phospholipid bilayer membranes induced by uncoupling agents for oxidative phosphorylation. *Proc. Nat. Acad. Sci.* **59**:484.
- Lea, E. J. A., Croghan, P. C. 1969. The effect of 2,4-dinitrophenol on the properties of thin phospholipid films. *J. Membrane Biol.* **1**:225.
- LeBlanc, O. H. 1969. Tetraphenylborate conductance through lipid bilayer membranes. *Biochim. Biophys. Acta* **193**:350.
- Lieberman, E. A., Babakov, A. V. 1968. Diminishing characteristics and impedance of phospholipid membranes in presence of tetrachlorotrifluorobenzimidazole. *Biofizika* **13**:362.
- Mochova, E. N., Skulachev, V. P., Topaly, V. P. 1968. Effect of uncoupling agents of oxidative phosphorylation on bimolecular phospholipid membranes. *Biofizika* **13**:188.
- Topaly, V. P. 1968*a*. Selective transport of ions through bimolecular phospholipid membranes. *Biochim. Biophys. Acta* **163**:125.
- — 1968*b*. Transfer of ions across bimolecular membranes and classification of uncouplers of oxidative phosphorylation. *Biofizika* **13**:1025.
- — 1969. Permeability of bimolecular phospholipid membranes for fat-soluble ions. *Biofizika* **14**:452.
- Markin, V. S., Krishtalik, L. I., Liberman, E. A., Topaly, V. P. 1969*a*. Mechanism of conductivity of artificial phospholipid membranes in the presence of ion carriers. *Biofizika* **14**:256.
- Pastushenko, V. F., Krishtalik, L. I., Liberman, E. A., Topaly, V. P. 1969*b*. Membrane potential and short circuit current in artificial phospholipid membranes in the presence of agents uncoupling oxidative phosphorylation. *Biofizika* **14**:462.
- Mitchell, P. 1966. Chemiosmotic coupling in oxidative and photosynthetic phosphorylation. *Biol. Rev.* **41**:445.
- Mueller, P., Rudin, D. O. 1969. Translocators in biomolecular lipid membranes: their role in dissipative and conservative bioenergy transducers. *In: Current Topics in Bioenergetics*, vol. 3. D. R. Sanadi, editor. p. 157. Academic Press, New York.
- Pangborn, M. C. 1951. A simplified purification of lecithin. *J. Biol. Chem.* **188**:471.
- Skulachev, V. P., Sharaf, A. A., Liberman, E. A. 1967. Proton conductors in the respiratory chain and artificial membranes. *Nature* **216**:718.